Journal of Neural Engineering

PAPER

Motor unit drive: a neural interface for real-time upper limb prosthetic control

To cite this article: Michael D Twardowski *et al* 2019 *J. Neural Eng.* **16** 016012

J. Neural Eng. 16 (2019) 016012 (15pp) https://doi.org/10.1088/1741-2552/aaeb0f

Motor unit drive: a neural interface for real-time upper limb prosthetic control

Michael D Twardowski[1,2], Serge H Roy[1,3], Zhi Li[2], Paola Contessa[1], Gianluca De Luca[1] and Joshua C Kline[1,4]

[1] Delsys Inc. and Altec Inc., Natick, MA, United States of America
[2] Department of Robotics Engineering, Human Inspired Robotics Laboratory, Worcester Polytechnic Institute, Worcester, MA, United States of America
[3] Sargent College of Health & Rehabilitation Sciences at Boston University, Boston, MA, United States of America

E-mail: jkline@delsys.com

Received 30 May 2018, revised 18 October 2018
Accepted for publication 24 October 2018
Published 12 December 2018

Abstract

Objective. Modern prosthetic limbs have made strident gains in recent years, incorporating terminal electromechanical devices that are capable of mimicking the human hand. However, access to these advanced control capabilities has been prevented by fundamental limitations of amplitude-based myoelectric neural interfaces, which have remained virtually unchanged for over four decades. Consequently, nearly 23% of adults and 32% of children with major traumatic or congenital upper-limb loss abandon regular use of their myoelectric prosthesis. To address this healthcare need, we have developed a noninvasive neural interface technology that maps natural motor unit increments of neural control and force into biomechanically informed signals for improved prosthetic control. *Approach.* Our technology, referred to as motor unit drive (MU Drive), utilizes real-time machine learning algorithms for directly measuring motor unit firings from surface electromyographic signals recorded from residual muscles of an amputated or congenitally missing limb. The extracted firings are transformed into biomechanically informed signals based on the force generating properties of individual motor units to provide a control source that represents the intended movement. *Main results.* We evaluated the characteristics of the MU Drive control signals and compared them to conventional amplitude-based myoelectric signals in healthy subjects as well as subjects with congenital or traumatic trans-radial limb-loss. Our analysis established a vital proof-of-concept: MU Drive provides a more responsive real-time signal with improved smoothness and more faithful replication of intended limb movement that overcomes the trade-off between performance and latency inherent to amplitude-based myoelectric methods. *Significance.* MU Drive is the first neural interface for prosthetic control that provides noninvasive real-time access to the natural motor control mechanisms of the human nervous system. This new neural interface holds promise for improving prosthetic function by achieving advanced control that better reflects the user intent. Beyond the immediate advantages in the field of prosthetics, MU Drive provides an innovative alternative for advancing the control of exoskeletons, assistive devices, and other robotic rehabilitation applications.

Keywords: motor unit, neural interface, prosthetic control, real-time sEMG decomposition

(Some figures may appear in colour only in the online journal)

[4] Author to whom any correspondence should be addressed.

Introduction

Beginning with the introduction of electrically powered prostheses more than 65 years ago (Reiter 1948) surface electromyographic (sEMG) signals recorded from residual muscles in amputated limbs have served as the primary source of neural information for myoelectric prosthetic control (Schultz and Kuiken 2011, Fougner *et al* 2012). The majority of these devices use one or more recording electrodes to translate the sEMG signal amplitude into voltage signals that drive the mechanical components of the prosthesis. In so doing, users are able to directly control the direction of prosthetic actuation by activating different muscles of their residual limb (Fougner *et al* 2012). However, previous scientific investigations have shown that the amplitude of the sEMG signal is only an approximation of the intended proportional increments of neural control that are nonlinearly related to the actual force of the contracting muscle (Milner-Brown and Stein 1975, Lawrence and De Luca 1983, Basmajian and De Luca 1985, Solomonow *et al* 1990, Solomonow *et al* 1991). Consequently, in spite of decades of use, amplitude-based myoelectric control methods remain prone to generating disproportional, highly variable control signals (Guanglin *et al* 2010, Schultz and Kuiken 2011) likely contributing to the relatively high-incidence of upper-limb myoelectric prosthesis abandonment—estimated at 23% of adults and 32% of children with major limb-loss (Biddiss and Chau 2007).

To improve neural interfaces beyond the limitations of amplitude-based myoelectric approaches, recent work has focused on advancing electrodes that can be implanted within muscles (Pasquina *et al* 2015) or on peripheral nerves to better access the underlying signals within the nervous system (Rossini *et al* 2010). In recent years, several of these implantable technologies have shown promise for recording signals for up to 12–24 months in cats and monkeys (Schorsch *et al* 2008, Baker *et al* 2010) and up to 6–9 months in human subjects (Pasquina *et al* 2015). Yet, despite these technical achievements, practical questions surrounding the implantation and maintenance of invasive neural interfaces remain, including: (1) the preservation of residual nerve or muscle integrity; (2) the management of increased health-risks to an aging population of people with limb-loss; and (3) the accommodation of substantially greater health costs by the prosthesis care system (Baker *et al* 2010, Schultz and Kuiken 2011, Lewis *et al* 2013, Pasquina *et al* 2015). Even if some of these practical concerns are mitigated over time, there remains an immediate need for a risk-averse neural interface that can provide comparable access to the motor control information within the nervous system, but in a noninvasive configuration.

To meet this need, we have developed a new neural interface technology, referred to as motor unit drive (MU Drive), to provide control signals that are based on the firing behavior of individual motor units obtained both noninvasively and in real-time. Motor unit firing rates and recruitment provide natural physiological mechanisms for controlling force and movement in the intact limb (De Luca and Erim 1994) and therefore hold promise for more natural restoration of function for persons with limb-loss. Our group has been at the forefront of developing algorithms for extracting motor unit firings from the decomposition of sEMG signals; first using intramuscular electrodes (LeFever and De Luca 1982, LeFever *et al* 1982, De Luca and Adam 1999) and more recently using high-fidelity noninvasive surface electrodes (De Luca *et al* 2006, 2014). This work has culminated in a system of sensors and algorithms that can measure the firing behavior of well over 20 motor units per contraction during exercise and functional human movements (De Luca *et al* 2014). In the current study, we developed and tested MU Drive on amputees with congenital or traumatic trans-radial limb-loss and found that sEMG signals obtained from residual muscles are not only decomposable, but the extracted motor unit activity provides valuable control information that incorporates known control properties documented in muscles of intact limbs. We combined the motor unit firings with the force generating properties of individual motor units to derive a biomechanically informed signal (MU Drive signals) that can be used as a control input for upper-limb prosthetic devices. We compared the characteristics of MU Drive signals to conventional amplitude-based signals in both trans-radial amputees as well as intact control subjects during various intended and actual movements of the hand, respectively. Across all subjects and movements tested, MU Drive signals provided more responsive and smoother real-time proportional control that better replicated actual movement of the limb.

Methods

Participants

A total of 23 subjects volunteered for participation: 13 subjects were amputees with trans-radial limb loss (four congenital and nine traumatic; eight males and four females; mean age 47.2 ± 15.1 years (range 26–74 years); mean residual limb length 14.1 ± 6.6 cm (range 7.5–32 cm))—and ten subjects were controls with intact limbs (five males and five females; mean age 37.4 ± 15.3 years (range 22–68 years)). All subjects were otherwise healthy and showed no signs of neuromuscular disorders. Each subject read, indicated they understood and signed informed consent forms approved by the Western Institutional Review Board before participating in the study.

Data acquisition

For both amputee (figure 1(A)) and control subjects (figure 1(B)), we recorded sEMG signals using a dEMG 5-pin surface array (Delsys Inc., Natick, USA) placed on the surface of the skin over each of four muscles—Extensor Digitorum Communis, Flexor Digitorum Profundus, Pronator Teres and the Biceps Brachii—associated with four intended and actual movements of the intact limb for amputees and control subjects: extension of the fingers, flexion of the fingers, pronation of the forearm and supination of the forearm, respectively. The sensors were placed over the mid-belly of each muscle, located by manual palpation and verified by sEMG signal monitoring during each of the specified intended or actual movements. At each sensor location, only mild skin preparation was performed by shaving excess hair with a razor, removing the superficial dead skin with medical-grade tape peels, and cleansing the skin with an alcohol swab. From each sensor, four differential sEMG signals were recorded from different bipolar pairs of the five-pin electrode, filtered from 20 to 450 Hz, and digitized at 20 kHz using a Bagnoli™ 16-channel EMG acquisition system (Delsys Inc.).

For control subjects, a custom data acquisition glove was used to accurately measure kinematics of the hand and forearm during the different movement tasks. The glove measured joint angles of each digit using five biaxial goniometers (Biometrics Ltd, Newport, UK) with Trigno™ Goniometer Adapters (Delsys Inc.) and forearm orientation using a Trigno™ IM inertial measurement sensor (Delsys Inc.). All primary goniometer axes were low-pass filtered at 50 Hz and digitized at 1.93 kHz. The triaxial gyroscope, accelerometer and magnetometer of the inertial sensor were digitized at 148.1 Hz, and processed using a custom orientation filter (Madgwick *et al* 2011) to provide three principal axes of roll, pitch and yaw. Trigger modules were used to synchronize the start and stop of data acquisition between the Bagnoli™ and Trigno™ systems. Data were acquired on a computer with an Intel® Core™ i7-4790 CPU @ 3.60 GHz with 8 GB of RAM and processed using custom MATLAB software.

Protocol

We designed a protocol to test voluntary intended and actual control of the hand in two degrees of freedom: (1) finger flexion/extension, and (2) forearm supination/pronation. For each degree of freedom, subjects started by performing a brief voluntary contraction at a relatively low-level, typical of normal daily activity. The signal-to-noise ratio of the recorded sEMG signal was monitored to prevent noise from obscuring the recognition of motor unit action potentials during the MU Drive processing described later in the methods. The sensor was removed and retested in multiple locations on the muscle until an sEMG signal-to-noise ratio of at least 4:1 could be obtained from the relatively low-level voluntary effort. Subjects then performed a brief 10–20 s initialization contraction of sufficient duration to extract the action potentials of approximately 20–30 different motor units during the motor unit action potential detection stage of MU Drive processing. Following initialization, subjects were instructed to perform a series of sequential trials of alternating contractions of finger flexion and extension and forearm pronation and supination through their full range of motion for approximately 12 to 24 repetitions. We tested each contraction at speeds of 20 and 40 repetitions per minute, to assess our algorithms viability during varied movement speeds within the bounds of normal daily activity. In both amputee and control subjects, sEMG biofeedback was visualized on a computer screen to facilitate compliance with the protocol. Additionally, amputee subjects simultaneously performed mirrored movements with the intact limb to assist themselves in activating the muscles involved in the intended movements. Rest periods were provided between each series of contractions to avoid the onset of muscle fatigue.

MU Drive processing

The sEMG signals recorded during the different movement tasks were processed to measure the firings of concurrently active motor units in real-time and convert the detected firing instances into a continuously varying biomechanically informed signal (figure 2). The approach is based on existing algorithms that use an offline architecture to measure motor unit firing times from sEMG signals recorded during dynamic exercise and functional movements (De Luca *et al* 2014). However, because the current post-processing architecture prevents real-time access to neural control signals, we implemented the following changes to develop real-time processing capabilities for the MU Drive algorithms.

Motor unit action potential detection. The existing dEMG algorithms identify action potentials of individual motor units by searching the recorded sEMG signal for uncontaminated occurrences of each action potential shape prior to resolving the motor unit firing locations. In the MU Drive algorithms, we separated this processing stage from the rest of the algorithm to detect *a priori* measurements of motor unit action potentials (MUAPs) during relatively brief contractions performed during the initialization stage for each sensor location (figure 2(A)). The detected MUAP shapes were parameterized within a multi-dimensional shape-based feature set used throughout later processing stages to track the firings of individual motor units. (See De Luca *et al* (2014) for further details.) This initialization step was performed at the onset of testing and the identified MUAP shapes were tracked throughout the remainder of the protocol without the need for re-calibration.

Real-time processing of motor unit firing times. The detected MUAP shapes were used to resolve motor unit firings that occurred in superposition with those of other motor units throughout the voluntary contractions. In the existing algorithms this stage requires processing the entirety of the recorded signal to resolve the firings of all motor units prior to outputting the result. To alleviate this computational burden, we parsed the sEMG data into smaller, non-overlapping signal segments and measured the firing locations of different motor units separately from each segment (figure 2(B)). To improve the firing time detection from relatively smaller duration signal segments, signal-based features extracted from occurrences of one or more motor unit action potentials that overlapped with a previous segment were used to inform the current segment processing. This implementation allowed us to reduce the overall processing delay by providing firing times as they are detected in the sEMG signal. (See De Luca *et al* (2006, 2014) and Nawab *et al* (2010) for further details.)

Translating motor unit firings into biomechanically informed signals. The existing dEMG algorithm provides the action potentials and firing times of all detected motor units. For the MU Drive algorithms, however, we designed an additional processing stage to translate the motor unit firing times into

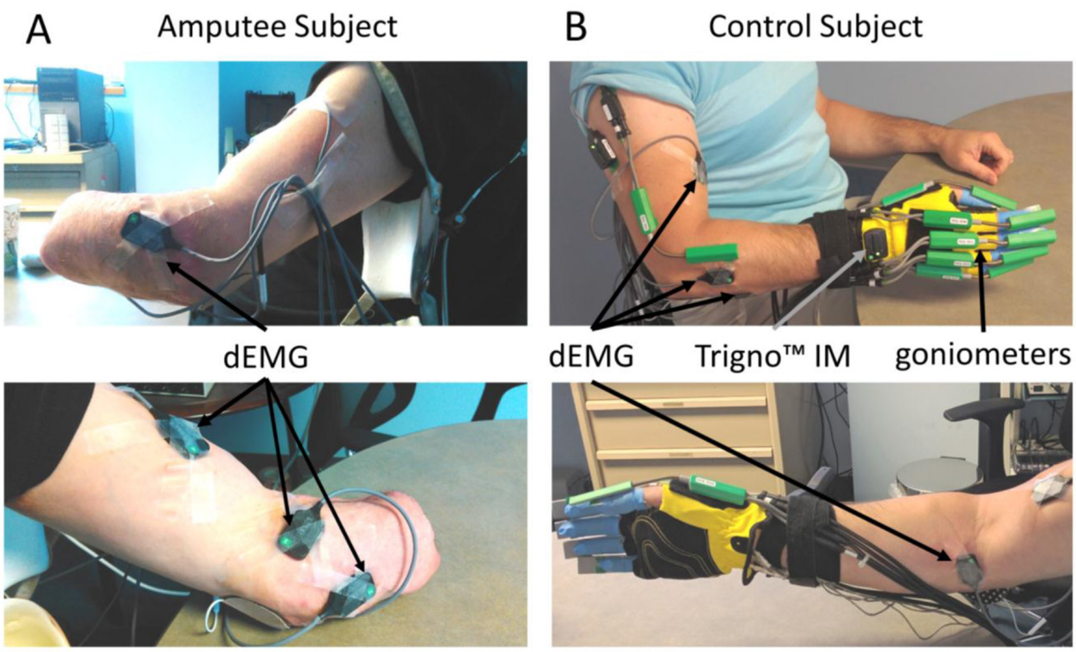

Figure 1. Examples of the experimental setup for one of the amputee (A) and control (B) subjects. EMG sensors are identified on the extensor digitorum communis, flexor digitorum profundus, pronator teres and the biceps brachii muscles to record surface electromyographic signals during the test protocol. The control subject is instrumented with a custom data acquisition glove comprised of goniometers, and an inertial measurement unit sensor to measure hand and forearm kinematics.

proportionally varying increasing and decreasing biomechanically informed signals. This component of the algorithm uses a specially designed neuromuscular transfer function to estimate the relative mechanical contribution of each active motor unit. While other approaches (Farina *et al* 2017) have attempted to pool motor unit firings with non-linear transforms of the sEMG signal to infer joint kinematics, we chose to directly model the biomechanical contributions of each firing of the individual motor units based on known and documented empirical measures of motor unit force twitches. The neuromuscular transfer function is adapted from an existing computational model of empirically-derived motor unit force twitches (Raikova and Aladjov 2002, Contessa and De Luca 2013) to obtain a signal representation of MU Drive from each muscle. Additional details of this procedure can be found in appendix A.

Data analysis

To assess the control characteristics of the MU Drive neural interface, we evaluated three primary signal metrics from each subject and muscle tested:

(1) *Real-time Performance*—We measured the total time required to obtain the output signal as the sum of the segmentation delay (i.e. the time required to record each signal segment) and the processing delay (i.e. the time required to obtain the output signal from each input signal segment). To evaluate the effects of window size on real-time performance, we segmented the sEMG data into windows ranging from 20 to 400 ms.
(2) *Proportional Smoothness*—We quantified the degree of smoothness of the output signal based on the spectral arc length (SPARC) described by Balasubramanian *et al* (2015). The SPARC measurement provides an indication of the smoothness of a movement based on the arc length of the discrete Fourier transform derived from a kinematic or biomechanical signal. This approach has been shown to provide valuable quantification of the smoothness of natural limb movement and thus provides a mathematical framework that can be used for assessing the smoothness of an input signal for prosthetic control.
(3) *Replication of Actual Limb Movement*—In control subjects, we chose to compare the MU Drive signals—obtained from the summation of force twitches produced from individual motor unit firings—to the kinematics (e.g. position, and orientation) of the hand and forearm as both force and position measures are inter-related and the estimate of either can used to be control the velocity of a prosthesis motor in a proportional manner (Fougner *et al* 2012). To make these comparisons, we quantified the degree to which the output signal replicates movement of an intact limb by calculating the percent error between each signal and the measured changes of the finger joint angle or forearm orientation indicated by the primary axis of roll. Each percent error was measured at the point of maximum cross correlation between the control signal and the appropriate kinematic measure.

Comparison with conventional amplitude-based myoelectric signals. We compared the MU Drive signal characteristics with the root mean square (RMS), and mean absolute value (MAV) of the sEMG signal that are typically used for amplitude-based myoelectric prosthetic control (Phinyomark *et al* 2012). These signals were calculated over a temporal window

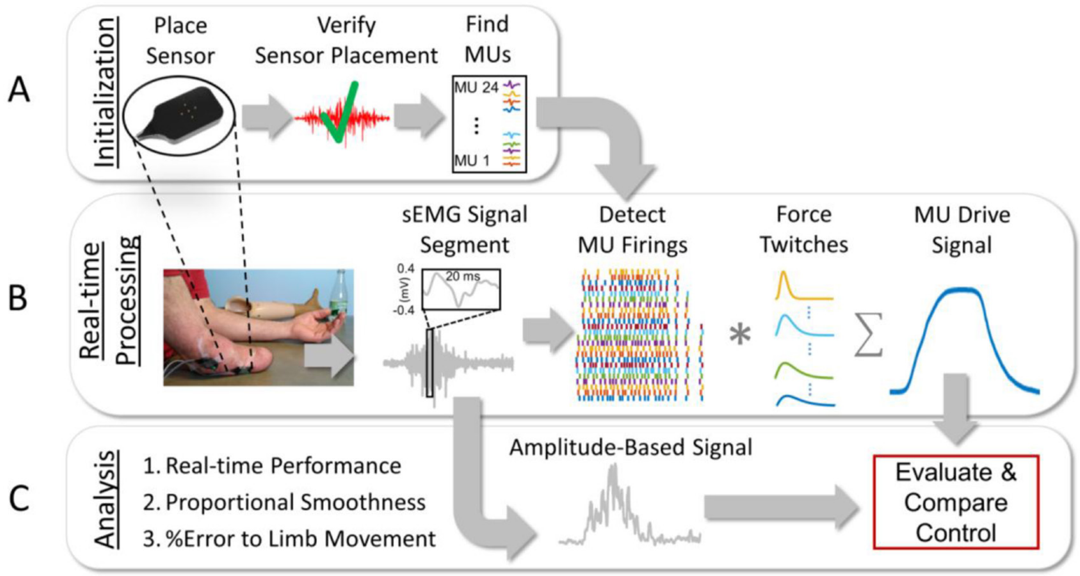

Figure 2. A schematic diagram of the MU Drive processing stages (A)–(C) used to detect and translate motor unit firings in real-time into biomechanically informed signals. (A) The first stage verifies sensor placement and acquires *a priori* measurements of the motor unit action potentials (MUAPs) from an initial brief contraction (in this example data is shown from the finger extensors from a control subject during finger flexion/extension). (B) The detected MUAPs are used to resolve motor unit firings in real-time which are then translated into the MU Drive signal using a neuromuscular transfer function that convolves the motor unit firing instances with model estimates of muscle force twitch. (C) The characteristics of the MU Drive signal were analyzed and compared to those measured from signals derived using conventional amplitude-based measures of the signal.

equal in duration to the total time required to obtain a MU Drive signal. For example (figure 2(C)), if the MU Drive output required a 20 ms segmentation delay and 5 ms processing time totaling a delay of 25 ms, then the amplitude-based signals would be calculated using an equivalent window size of 25 ms. The amplitude-based myoelectric signals, MU Drive signals, and kinematic data were normalized for each subject and movement direction prior to the analysis. We measured the latency of each amplitude-based signal with respect to the MU Drive signal by finding the point of maximum cross correlation between the two signals. The latency, smoothness and error metrics were analyzed for all signals as a function of different window lengths. A non-parametric Wilcoxon rank sum test was used to evaluate significant differences between the MU Drive and the amplitude-based signals.

Results

We successfully measured the motor unit firing behavior from 4942 volitional and intended contractions in all 23 subjects tested. On average, the MU Drive real-time performance achieved 2.7 ± 1.3 ms (5th and 95th Percentiles $= 0.7, 4.7$ ms) processing time for each 20 ms signal segment, equivalent to a real-time ratio less than 0.25:1 and upper-limit total delay of approximately 25 ms. When we compared the MU Drive signal measured from each muscle with that of the amplitude-based signals obtained with a comparable 25 ms delay (i.e. 25 ms window) from the same muscle, we observed that MU Drive improves the control characteristics shown by the representative examples in figure 3.

The MU Drive signal measured from the forearm pronator in the amputee subject during intended forearm pronation/supination maintained a smoothness of -6.0 (figure 3(A), black), a 97.4% improvement relative to the -232.0 smoothness measured from the RMS signal (figure 3(A), gray). Similarly, in the control subject during finger extension/flexion, the MU Drive signal measured from the finger extensors had a smoothness of -6.5 (figure 3(B), black), a 97.6% improvement relative to the -275.5 smoothness measured from the RMS signal (figure 3(B), gray) and closer to the -6.6 smoothness measured from the changes in finger angle of the control subject's intact limb (figure 3(B), black dashes).

When comparing the measured changes in joint angle of the 2nd finger of the control subject with the MU Drive and RMS signals measured from the finger extensors, we found that MU Drive was able to better replicate changes in movement of the intact limb with a relatively small error of 8.0% (figure 3(B), black), substantially lower than the 57.8% error measured from the RMS signal (figure 3(B), gray).

We compared the performance characteristics of MU Drive and RMS signals in both the amputee and control subjects for all muscles and movements tested. Figure 4 shows examples of individual results selected to illustrate the varying degrees of performance. In these examples, the MU Drive signals ranged in smoothness from -8 to -4.4 and from -16.6 to -6.0, substantially greater than the smoothness of the RMS signals which ranged from -203.2 to -38.7 and from -239.7 to -107.8 for amputee and control subjects, respectively. Similarly, the error measured between the MU Drive signals and the actual limb movement of the control subjects ranged

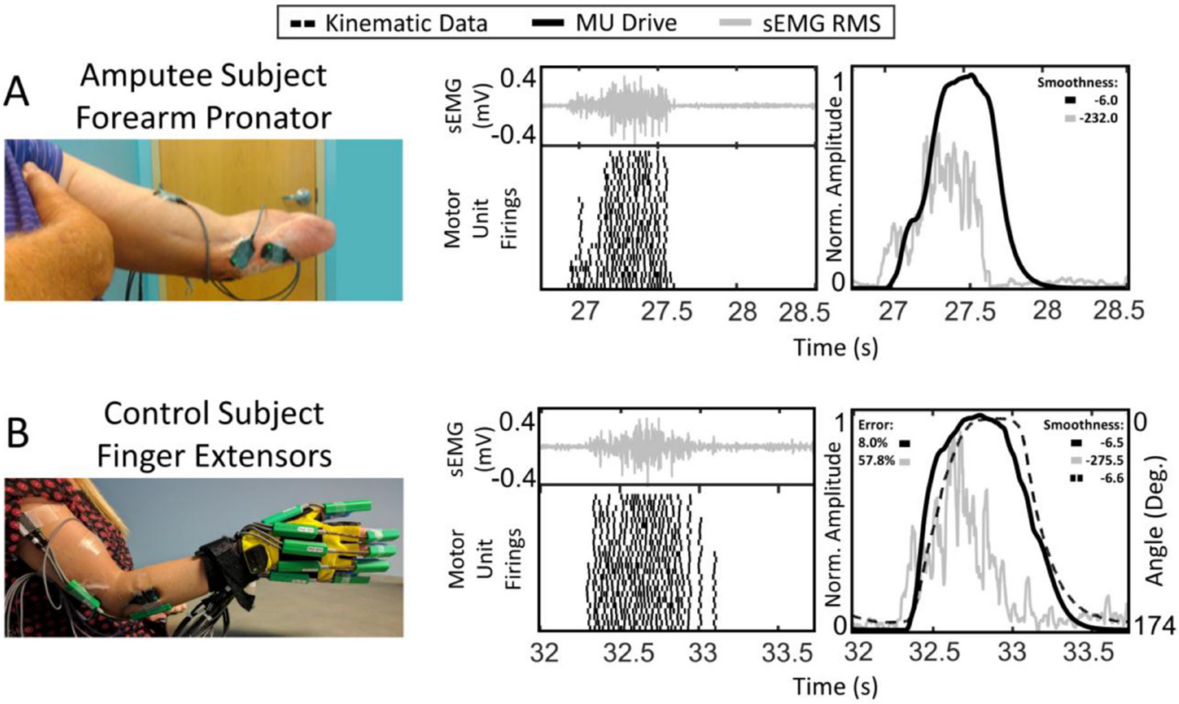

Figure 3. (A) The sEMG signal (left-top, gray), the detected motor unit firings (left-bottom, black), MU Drive signal (right, black) and RMS signal (right, gray) measured from the forearm pronator during intended forearm pronation/supination of a representative amputee (subject A2). (B) Both MU Drive and RMS signals are plotted with the joint angle of the 2nd finger (right, black dashes) measured during finger flexion/extension from the finger extensor muscles of a representative control (subject C2). MU Drive consistently provides smoother signals that better replicate intended limb movement than the RMS signals.

from 19.1% to 23.9%, substantially lower than the error measured between the RMS signals and the actual limb movement which ranged from 62.9% to 82.6%. In all cases, MU Drive provided smoother signals than RMS signals and better replicated actual limb movement in control subjects.

MU Drive provides smoother signals

We segmented the sEMG signals at different window lengths to analyze the changes in the MU Drive and amplitude-based signal characteristics as a function of the window size and processing time required to obtain each signal. Results from amputee subjects indicate that the median smoothness of MU Drive manifested relatively small fluctuations with increasing delay, ranging from −7.0 to −6.1 in the finger flexors (figure 5(A)), −11.5 to −7.7 in the finger extensors (figure 5(B)) during finger extension/flexion, and −10.3 to −8.4 in the forearm supinator (figure 5(C)), and −5.1 to −4.4 in the forearm pronator (figure 5(D)) during forearm supination/pronation. This contrasts with the median smoothness of the amplitude-based signals measured from the same muscles that progressively increased as a function of window size and processing time to a maximum smoothness of −111.6 (RMS) and −43.2 (MAV) in the finger extensors (figure 5(A)), −98.2 (RMS) and −52.1 (MAV) in the finger flexors (figure 5(B)), −75.3 (RMS) and −33.1 (MAV) in the forearm supinator (figure 5(C)), and −113.4 (RMS) and −36.8 (MAV) in the forearm pronator (figure 5(D)). In spite of the apparent improvement for each movement, the best amplitude-based smoothness metrics were all significantly lower than the smoothness of the MU Drive signals obtained with the least delay at 25 ms ($p < 0.001$). Similar results can be seen from control subjects, where the MU Drive signals showed relatively small fluctuations that ranged from −9.4 to −7.2 in the finger extensors (figure 5(E)), and −11.2 to −9.3 in the finger flexors (figure 5(F)) during finger extension/flexion, and −9.0 to −7.5 in the forearm supinator (figure 5(G)), and −11.7 to −8.5 in the forearm pronator (figure 5(H)) during forearm supination/pronation. This contrasts with the median smoothness of the amplitude-based signals measured from the same muscles which progressively increased as a function of window size and processing time up to −97.4 (RMS) and −29.6 (MAV) in the finger extensors (figure 5(E)), −111.7 (RMS) and −42.2 (MAV) in the finger flexors (figure 5(F)), −46.3 (RMS) and −27.8 (MAV) in the forearm supinator (figure 5(G)), and −60.3 (RMS) and −21.8 (MAV) in the forearm pronator (figure 5(H)). Like the amputee subjects, the best amplitude-based smoothness for each muscle and movement tested in control subjects was significantly lower than the smoothness of the MU Drive signals obtained with 25 ms delay ($p < 0.001$). The smoothness measured from kinematics of the limb in control subjects during each movement was −4.6 in the finger extensors (figure 5(E)), −5.5 in the finger flexors (figure 5(F)), −4.9 in the forearm supinator (figure 5(G)), and −3.9 in the forearm pronator (figure 5(H)). These data indicate the smoothness of the MU Drive signals is relatively closer than the amplitude-based signals to the smoothness measured from movement of the actual limb.

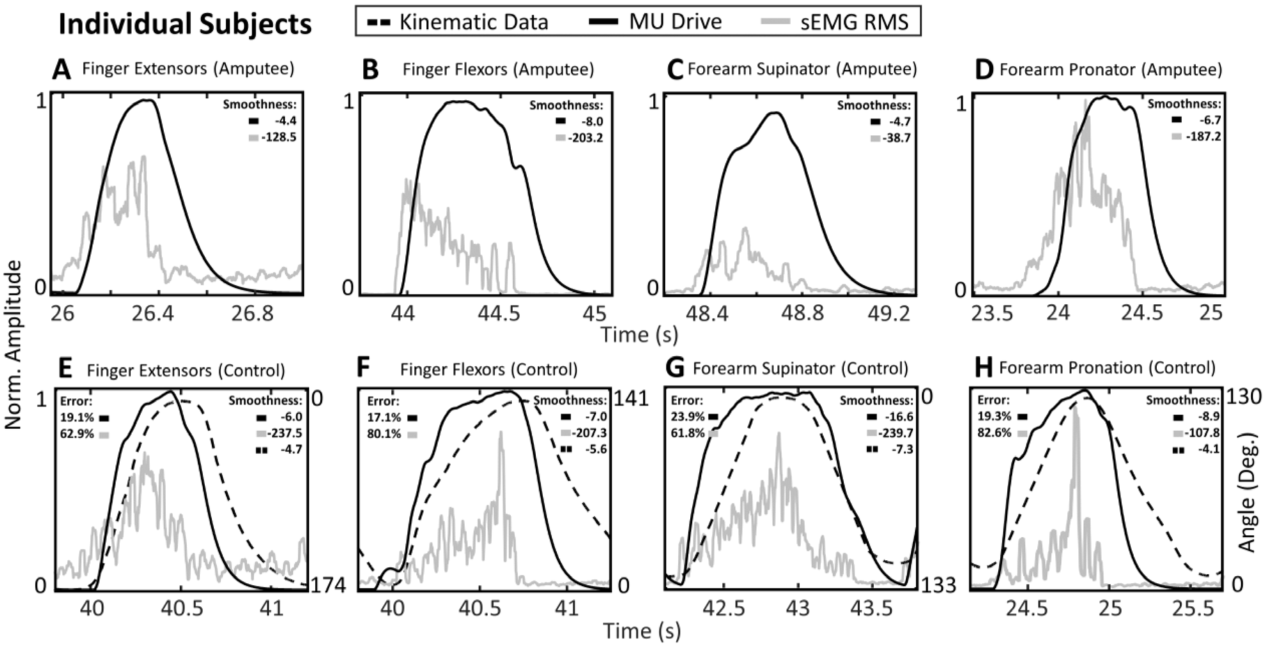

Figure 4. MU Drive signals (black) compared to RMS signals (gray) measured from the finger extensors (A) and (E), the finger flexors (B) and (F), the forearm supinator (C) and (G) and the forearm pronator (D) and (H) of amputee ((A)–(D), subjects: A2, A3, A4, A5) and control subjects ((E)–(H), subjects: C2, C3, C4, C5) during finger flexion/extension ((A), (B), (F) and (E)), forearm pronation/supination ((C), (D), (G) and (H)). MU Drive provides similar performance across the subjects and muscles tested.

Because there were no systematic differences in smoothness amongst the individual subjects, we grouped the smoothness data across all amputee subjects and separately across all control subjects for each muscle tested. We analyzed the smoothness measured from the amplitude-based signals across the full-range of window lengths tested as a function of the latency with respect to the MU Drive signal obtained with 25 ms delay. (Note that negative latencies indicate the amplitude-based signal leads MU Drive while positive latencies indicate that the amplitude-based signal lags behind MU Drive.) Across all four muscles the median smoothness of movement of MU Drive ranged from −8.4 to −6.9 (figures 6(A)–(D)) and −11.7 to −10.5 (figures 6(E)–(H)) for the amputee and control subjects, respectively. These values were significantly greater ($p < 0.001$) than the best median smoothness of the RMS signals which ranged from −117.0 to −68.1 for amputee (figures 6(A)–(D)) and from −108.5 to −53.5 for control subjects. Although the MAV window function improved over the smoothness of the RMS across all muscles tested, MU Drive was still significantly smoother ($p < 0.001$) than the best performing MAV signals which ranged from −49.5 to −31.7 for amputees (figures 6(A)–(D)) and from −42.7 to −26.5 (figures 6(E)–(H)) for control subjects. Further analysis of figure 6 illustrates that the smoothness of the RMS and MAV signals was directly related to the latency of the signals with MU Drive, indicating the best performing windows for both functions lagged behind MU Drive with median latencies ranging from 49 to 171 ms and from 76 to 143 ms for all muscles and subjects for RMS and MAV signals, and in most cases lagged behind the actual movement of the limb which had a median latency with respect to MU Drive that ranged from 61 to 159 ms (figures 6(E)–(H)). These data indicate that the smoothness of the amplitude-based measures can be improved, but at the expense of additional latency that results from increasing the window size.

MU Drive better replicates movement of intact limbs

We calculated the percent error between the MU Drive and amplitude-based signals with respect to the changes in joint angle during each movement of control subjects. Results from individual control subject indicate the median error of MU Drive manifested relatively small variations which ranged from 18.8% to 24.77% in the finger extensors (figure 7(A)) and 23.3% to 31.2% in the finger flexors (figure 7(B)) during finger extension/flexion, and 26.1% to 31.3% in the forearm supinator (figure 7(C)) and 24.5% to 31.2% in the forearm pronator (figure 7(D)) during forearm supination/pronation. On the contrary, the median error of the amplitude-based signals from the same muscles improved as a function of increasing window size and processing time reaching minimum values of 30.6% (RMS) and 33.3% (MAV) in the finger extensors (figure 7(A)), 34.5% (RMS) and 31.9% (MAV) in the finger flexors (figure 7(B)), 36.5% (RMS) and 31.8% (MAV) in the forearm supinator (figure 7(C)), and 57.0% (RMS) and 60.5% (MAV) in the forearm pronator (figure 7(D)). Yet even with this improvement, the minimum error measured from the amplitude-based signals for each muscle and movement studied was significantly greater than the error measured from the MU Drive signals at 25 ms delay ($p < 0.001$).

Because there were no systematic differences in the error measured from the individual subjects, we grouped the data across all control subjects for each muscle and movement tested and analyzed the error measured from the

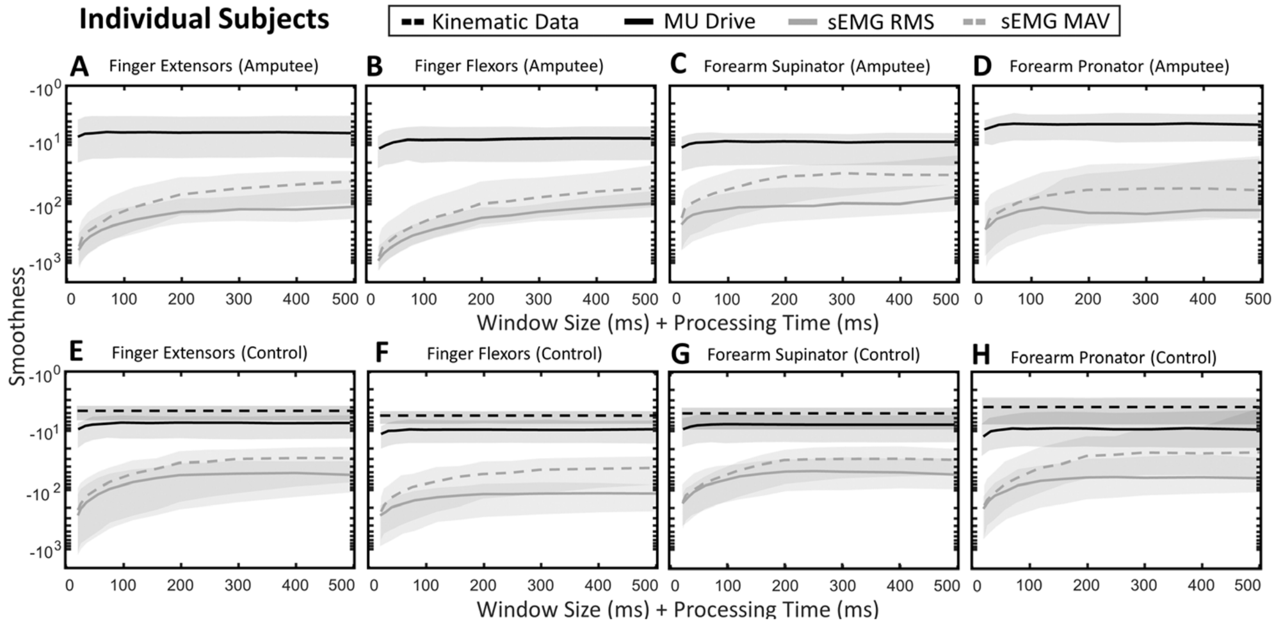

Figure 5. Smoothness measurements at different window lengths used to estimate and compare MU Drive (black), RMS signals (gray), and MAV signals (gray dashes) measured from the finger extensors (A) and (E), the finger flexors (B) and (F), the forearm supinator (C) and (G) and the forearm pronator (D) and (H) of amputee ((A)–(D), subjects: A1, A2, A3, A6) and control subjects ((E)–(H), subjects: C3, C6, C7) during finger extension/flexion ((A), (B), (E) and (F)) and forearm supination/pronation ((C), (D), (G) and (H)). The median smoothness values are represented by the solid traces, while the shaded regions represent the 5th to 95th percentiles. Across all subjects and muscles tested, MU Drive consistently provided smoother signals compared to the amplitude-based signals.

amplitude-based signals across the full range of window lengths tested as a function of latency with respect to the MU Drive signal at 25 ms delay. The median error of MU Drive was 22.8%, 25.9%, 25.6% and 34.3%, significantly lower ($p < 0.001$) than the measured median error of the RMS signals of 28.9%, 33.1%, 35.9% and 47.8% in the finger extensors, finger flexors, forearm supinator and forearm pronator, respectively (figures 8(A)–(D)). The median error of MU Drive was also significantly lower ($p < 0.001$) than the measured median error of the MAV signals of 30.1%, 40.4%, 38.3% and 51.6% in the same finger extensors, finger flexors, forearm supinator and forearm pronator muscles during the same movements tested. Importantly we observed the percent error of amplitude-based signals were inversely related to the latency of the response with respect to MU Drive: the best performing sEMG window length incurred median latencies ranging from 84 to 171 ms and 82 to 143 ms for RMS and MAV functions, respectively. These data give clear evidence that MU Drive signals are more responsive and more closely replicate the kinematics of the intact limb.

Discussion

We set out to design a new, noninvasive neural interface that uses the firings of individual motor units to derive a biomechanically informed signal that could be used as an input for prosthetic control. This study provides a critical proof-of-concept towards achieving this goal prior to actual implementation in a prosthesis. Our tests across four different muscles and as many movements established, for the first time, that the MU Drive neural interface is able to track the firings of individual motor units in both amputee and control subjects, and the detected firings could be successfully translated into time-varying biomechanically informed signals that were responsive, smooth and a close approximation of the actual movement of intact limbs. Additionally, our results demonstrate that residual muscles, despite disuse and changes to their morphology due to surgery or congenital formation, can still provide responsive, smooth, and proportional MU Drive signals that are similar in control characteristics as those measured from intact limbs. When comparing the characteristics of the MU Drive signals with traditional amplitude-based myoelectric signals, we found that MU Drive provided several significant improvements discussed in further detail below.

MU Drive provides smoother signals

As the activation of different muscles increased and decreased throughout the movements tested, the MU Drive signal provided proportional increases and decreases that were significantly smoother than changes in the amplitude-based signals. The relatively poorer smoothness of amplitude-based signals may contribute to the reason why current commercially available myoelectric prosthetic controllers rely on preset thresholds that limit proportional gradations of amplitude-based control. On the contrary, MU Drive extracts the relevant neural information from the variable electrical activity of the myoelectric signal by separating discrete motor unit control increments to provide a more natural, smooth and proportionally varying biomechanically informed signal. The end result demonstrates in both amputee and control subjects that MU Drive signals are closer in smoothness to the kinematics of actual movement of intact limbs (figure 5).

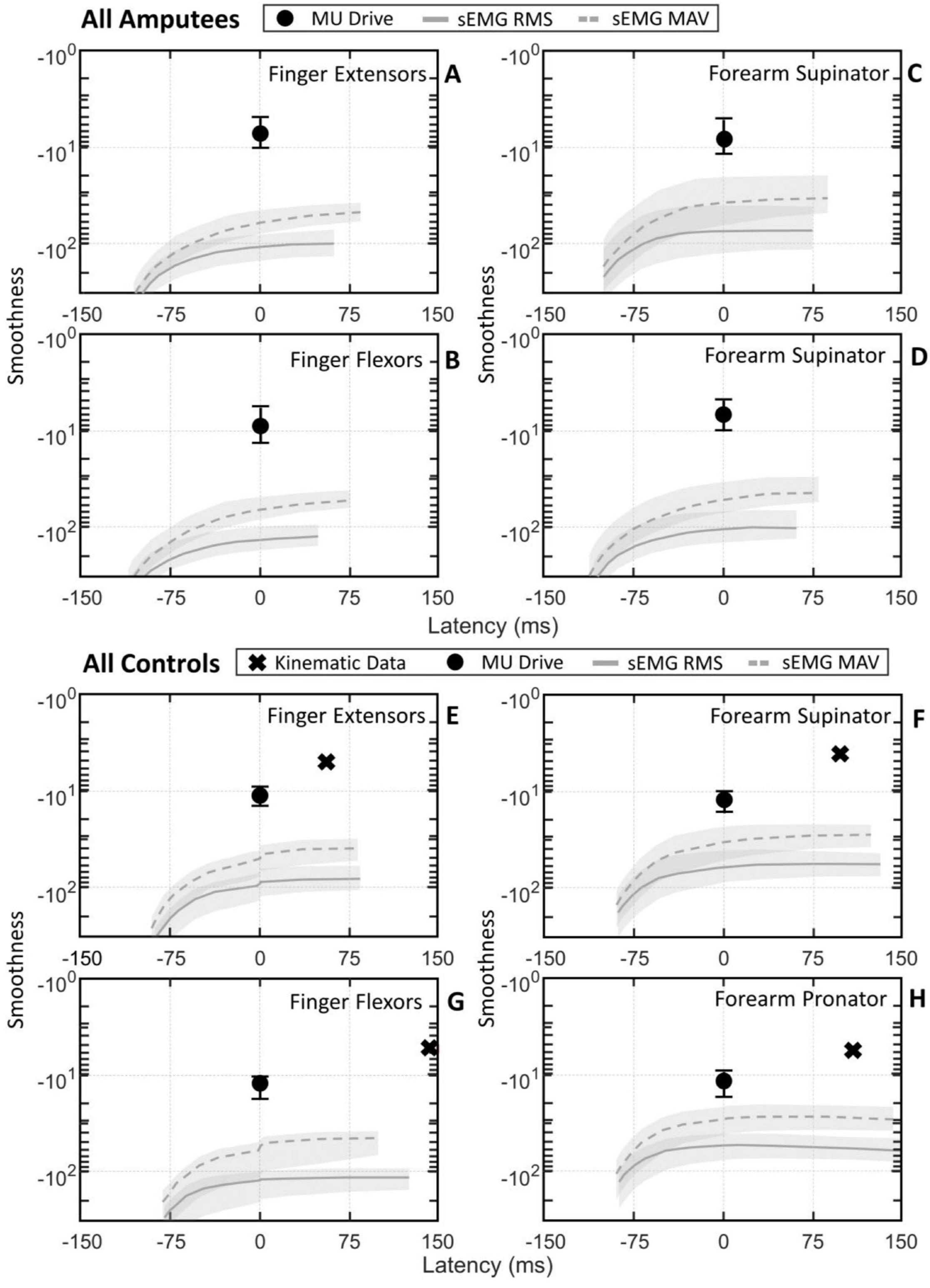

Figure 6. Smoothness measurements from RMS (gray), and MAV signals (gray dashes) plotted as function of median latency with respect to the MU Drive signal (black), measured from the finger extensors (A) and (E), the finger flexors (B) and (F), the forearm supinator (C) and (G) and the forearm pronator (D) and (H) of all amputee (A)–(D) and control subjects (E)–(H) during finger extension/flexion ((A), (B), (E) and (F)), forearm supination/pronation ((C), (D), (G) and (H)). Negative latencies indicate that a signal leads MU Drive, while positive latencies indicate that a signal lags it. The smoothness data from MU Drive signals at 25 ms delay are plotted as the median values (black circle) plus and minus the 25th and 75th percentiles (black error bars). For the control subjects ((E)–(H)) the smoothness measurements of kinematic data are plotted as the median values (black x) that spans the 25th and 75th percentiles at the *x*-axis corresponding to their median latency with the MU Drive signals (black). The median smoothness of the amplitude-based signals is represented by the solid traces, while the shaded regions indicate the 25th to 75th percentiles. Across all four muscles in both subjects sets, the MU Drive signals maintained significantly greater smoothness than the amplitude-based signals at every latency.

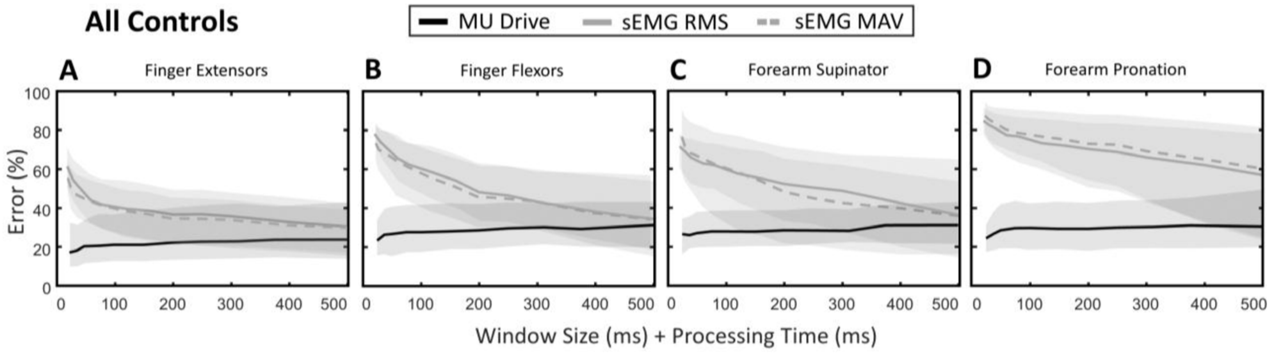

Figure 7. Error measurements at different window lengths used to estimate and compare MU Drive (black), RMS signals (gray), and MAV signals (gray dashes) measured from the finger extensors (A), the finger flexors (B), the forearm supinator (C) and the forearm pronator (D) of control subjects during (subjects: C3, C5, C8) finger extension/flexion (A) and (B), forearm supination/pronation (C) and (D). Median error values are represented by the solid traces, while the shaded regions represent the 5th to 95th percentiles. The MU Drive signals consistently provide significantly less error than the minimum error measured from the amplitude-based signals.

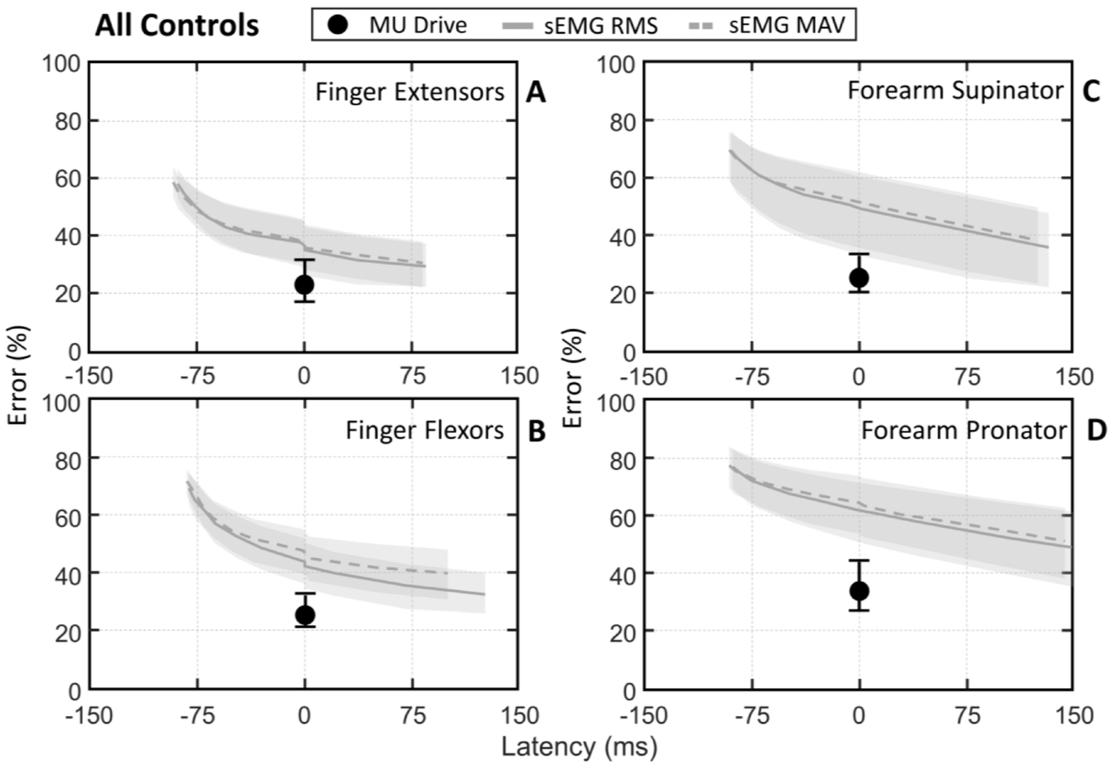

Figure 8. Error measurements from RMS signals (gray), and MAV signals (gray dashes) as a function of median latency with respect to the MU Drive signal (black), measured from the finger extensors (A), the finger flexors (B), the forearm supinator (C) and the forearm pronator (D) of all control subjects during finger extension/flexion (A) and (B), forearm supination/pronation (C) and (D). Negative latencies indicate that a signal leads MU Drive, while positive latencies indicate that a signal lags it. The error data from MU Drive signals at 25 ms delay are plotted as the median values (black circle) plus and minus the 25th and 75th percentiles (black error bars). The median errors of the amplitude-based signals are represented by the solid traces, while the shaded regions represent the 25th to 75th percentiles. Across all four muscles and at every latency the MU Drive signals maintained significantly less error than the amplitude-based signals.

MU Drive better replicates kinematics of intact limb

When compared to the kinematic changes in limb movement measured from control subjects, MU Drive provided significantly less error than the amplitude-based signals at all filtering windows tested. These results indicate that traditional amplitude-based myoelectric signals poorly replicate natural movement of the actual limb, perhaps contributing to the relatively high incidence of prosthesis abandonment among myoelectric prosthesis users (Biddiss and Chau 2007). To increase the accuracy of amplitude estimation, other approaches have been proposed to condition the sEMG signal prior to amplitude-based calculations (Clancy *et al* 2006, Liu *et al* 2013, Dai *et al* 2017). While these approaches have had some success in decreasing error of the amplitude estimates used for predicting torques of the elbow during constant-posture, force-varying contractions, their efficacy during dynamic human movements, such as those tested in this study, has yet

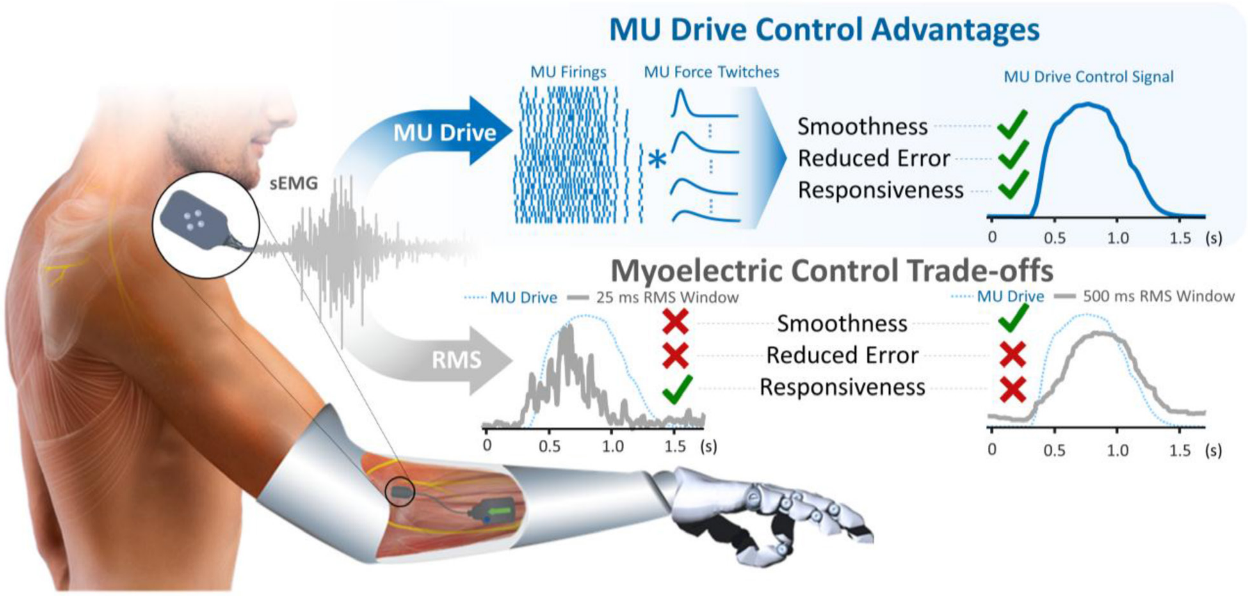

Figure 9. MU Drive control advantages over amplitude-based myoelectric control methods.

to be proven. In contrast to amplitude-based signals, MU Drive uses physiological mechanisms of motor unit-based control that capture natural changes in excitation from the nervous system translated by empirically-derived motor unit force twitch responses inherent to the muscle. The resulting biomechanically informed signals lead to more natural and faithful replication of actual limb movement that hold promise for improving precision and functionality of prosthetic controllers. Despite significantly improving the median error over amplitude-based signals, MU Drive retained some error with respect to the limb movement—likely resulting from the fact that normal voluntary movements of the hand typically result from not one but multiple synergist and antagonist muscles contributing to movement. Further investigation of multi-muscle mapping of MU Drive signals to movement patterns of the hand and arm will be an important step for improving MU Drive control of prosthetic devices in future research.

MU Drive provides responsive real-time processing

The improved signal characteristics of MU Drive required only a 25 ms delay in processing time and showed minimal changes in performance when testing increased delays from processing longer duration windows. The amplitude-based signals on the contrary showed an inherent tradeoff, illustrated in figure 9, between signal performance and processing time: increases in smooth signals that better replicate actual limb movement could be obtained from larger filtering windows that require increased delay to compensate for inherent variability in the myoelectric signal amplitude. This poses an inherent limitation in the degree of natural proportional control that can be obtained from amplitude-based signals while maintaining a 100–125 ms upper-limit responsiveness before the perceived delay affects the function of the prosthesis for users (Farrell and Weir 2007). Additional experimental testing of low-pass filtering techniques to improve performance the amplitude-based signals, shown in appendix B, further demonstrated the tradeoff between smoothness, latency and error inherent to amplitude-based myoelectric control methods. Furthermore, these results also demonstrated that it is feasible to aggressively low-pass filter amplitude-based signals to achieve comparable smoothness and latency to that of MU Drive (figure B1(X)), but at a compromise of increased error (figure B1(U)), that could translate into a reduced ability of prosthesis users to control a desired joint trajectory. Because MU Drive signals do not require significant filtering, they overcome the inherent tradeoff between performance and delay by providing smooth control that naturally replicates actual limb movement in a responsive configuration. In fact, the relatively low 25 ms delay of MU Drive increases its viability for integration with additional control algorithms that could combine multiple MU Drive signals across muscle synergies for increased multi-degree-of-freedom capabilities; thereby surpassing the current state-of-the-art while maintaining responsive performance.

These three improvements in the signal characteristics of MU Drive over conventional amplitude-based myoelectric alternatives establish a vital proof-of-concept for the functionality of our motor-unit-based neural interface. The advancements afforded by MU Drive justify further development and testing within a prosthesis to evaluate the degree to which the improved signal characteristics translate into natural, intuitive prosthetic control that could potentially increase function for a greater number of people with congenital or traumatic limb-loss.

Technical Advantages

The improved performance characteristics of MU Drive are supported by key aspects inherent to the engineering design of high-fidelity noninvasive sensors and real-time recognition algorithms. The technical attributes of the MU Drive system provide distinct advantages over alternative approaches for advancing prosthetic control.

MU Drive uses a miniaturized, noninvasive sensor. Our sensor design is unique among decomposition techniques in that it requires only a single, noninvasive, dry miniature sensor-array that allows discrimination of motor unit action potential shapes from sEMG signals. Because of its relatively small 5 × 5 mm electrode footprint, one or more of these arrays could be tailored for multi-muscle use within a prosthetic socket. In fact, prior work with similar sensors developed by our group found that those sensors were able to be integrated into a clinically available suction socket with only limited modifications (Hefferman *et al* 2014). This contrasts with alternative approaches for measuring motor unit firings that require relatively large patches of sensor arrays with as many as 64 electrodes that have difficulty maintaining consistent contact with the skin (Holobar *et al* 2009, Barone and Merletti 2013) even with the application of conductive gel paste to each of these electrodes. Although used in a limited set of bench-top laboratory conditions, the requirement for people with congenital or traumatic limb-loss to don these large arrays one or more times per day not only presents a practical burden to the user that will not only hinder compliance with the prosthetic device, but risk dermatological irritation caused by electrode gel on the already sensitive skin of the residual limb that ultimately depreciates the amputee's functionality with the prosthesis (Bowker and Michael 1992). In contrast, our MU Drive sensor's small form factor and dry-contact interface makes our system likely more amenable for future integration into the prosthetic socket with virtually no additional burden to the prosthesis donning procedure for the user.

MU Drive integrates real-time motor unit measurements. MU Drive presents the first noninvasive, high-yield, real-time implementation of sEMG decomposition algorithms for measuring motor unit firings. Real-time extraction of motor unit firings from the sEMG signal during voluntary movements provides responsive, proportional signals that are based on the natural physiological increments of force and movement. Prior attempts at real-time decomposition by other groups (Glaser *et al* 2013) in the field required approximately 600 ms of processing time for every 1 s of data to track a limited subset of up to four active motor units, during constrained stationary contractions. In contrast, our MU Drive algorithms measured the firing behavior of typically 20–30 motor units during non-stationary voluntary movements with only 5 ms delay for every 20 ms segment of data. The improved yield and computational processing of MU Drive provides responsive, data rich signal sources, which can be further integrated into existing prosthetic controllers or next-generation biomechanical control models while maintaining a responsive performance for prosthesis users.

MU Drive outputs biomechanically informed signals. By extracting motor unit firing times and translating them into biomechanically informed signals using motor unit force twitch estimates, MU Drive is able to provide a smooth, proportional signal that approximates the physiological changes in joint position produced by the natural force production of a muscle. This differs from conventional myoelectric approaches that use amplitude-based window filtering to infer, but not directly measure, how the electrical activation translates to mechanical output from a muscle. Consequently, current myoelectric prostheses are subject to the sources of variability inherent to the sEMG signal amplitude including noise in the signal baseline, the spatial filtering of MUAPs as the distances between motor units and recording electrodes change during voluntary contractions, among other factors (Basmajian and De Luca 1985, De Luca 1997). Because the biomechanically informed MU Drive output is based on discrete motor unit firings that are robust to these sources of electrical noise, MU Drive is able to better replicate natural physiological movements when compared to kinematic measurements from the intact limb.

Conclusion

MU Drive shows, for the first-time, that it is possible to measure, in real-time, the firings of individual motor units from a residual limb without sensor implantation on a nerve or within a residual muscle. The detected firing information can be convolved with mathematically derived motor unit force twitches to create biomechanically informed signals that promise more responsive, smooth, proportional control that better replicates the movement of intact limbs. By establishing this proof-of-concept, this study demonstrates the significant advantages of MU Drive over traditional amplitude-based myoelectric approaches and provides the foundation for motor-unit-based prosthetic controllers that can leverage multiple MU Drive control signals across muscle synergies to enable multi-degree-of-freedom upper-limb prosthetic control. These technological advancements signify a paradigm shift in the development of MU Drive neural interfaces to meet immediate health needs in the field of prosthetics and advance human-machine interfaces more broadly for exoskeleton control, assistive devices, and robotic rehabilitation.

Acknowledgments

We are grateful to Matt Albuquerque, CPO, and the staff at Next Step Bionics & Prosthetics, Inc. for useful discussion in planning the experiments and facilitating recruitment and data collection. Additional support in identifying appropriate subjects for this study was provided by Greig Martino, CP from United Prosthetics, Inc., the Amputee Coalition, and Dennis Amtower, CPO. We are grateful to all the subjects for their voluntary participation in the experiments, and for those with limb loss we thank them for the valuable insight they provided in guiding our research. The authors have confirmed that any identifiable participants in this study have given their consent for publication.

Research reported in this paper was supported in part by the De Luca Foundation, Delsys Inc., and by a grant from the National Institute of Neurological Disorders and Stroke under award number R43NS093651 and the Eunice Kennedy Shriver

National Institute of Child Health and Human Development under award number R44HD094626 of the National Institutes of Health.

Appendix A. Transformation of motor unit firings into biomechanically informed signals

To estimate the mechanical contribution of each active motor unit we adapted an existing computational model of empirically-derived motor unit force twitches computed as a function of time, the firing properties of each motor unit, and the motor unit firing history (Raikova and Aladjov 2002, Contessa and De Luca 2013). For each motor unit i, we modeled the force twitch profile $f_i(t)$ using three force twitch parameters as a function of motor unit size (figure 2(B)): amplitude (P_i) defined as the peak value, rise time ($T_{r,i}$) defined as the time from the beginning of the force twitch to the peak value, and half relaxation time ($T_{hr,i}$) defined as the time from the peak value to a point where the amplitude is one-half of the peak value

$$f_i(t) = pt^m e^{-kt} \tag{A1}$$

where p, m and k are obtained using:

$$p = P_i\left(\frac{e}{T_{r,i}}\right)^{kT_{r,i}} \tag{A2}$$

$$m = kT_{r,i} \tag{A3}$$

$$k = \frac{\ln(2)}{T_{hr,i} - T_{r,i}\ln\left(1 + \frac{T_{hr,i}}{T_{r,i}}\right)}. \tag{A4}$$

We tailored a set of generalized force twitch parameters from a range of empirical and simulated values listed in Contessa and De Luca (2013) using a genetic algorithm for physiologically realizable parametric optimization. These values resulted in P ranging from 1 to 1.5, T_r ranging from 70 to 90 ms, and T_{hr} ranging from 40 to 130 ms. In general, smaller motor units were modeled with longer rise times, longer half relaxation time, and lower peak force values than larger motor units. Gain factors $g_{ij}(fn_{ij})$ were calculated to attenuate sequential force twitches based on firing history of each motor unit, where IPI_{ij} indicates the inter-pulse interval between the jth and jth $-$ 1 firings of the ith motor unit, using the force twitch parameters of each motor unit and values $r = 0.85$ and $c = 2.13$ determined by Contessa and De Luca (2013)

$$g_{ij}(fn_{ij}) = \begin{cases} 1, & 0 < fn_{ij} \leqslant 0.4 \\ \frac{0.4}{fn_{ij}(1-r)}\left[1 - re^{\frac{0.4 - fn_{ij}}{c}}\right], & fn_{ij} > 0.4 \end{cases} \tag{A5}$$

where fn_{ij} is the normalized instantaneous firing rate of the jth firing of the ith motor unit found by:

$$fn_{ij} = \frac{T_{r,i}}{\mathrm{IPI}_{ij}}. \tag{A6}$$

Gain adjusted force twitch profiles were convolved with the firing instances of each motor unit from each window segment and summated across all active motor units to obtain a signal representation of the MU Drive from each muscle.

Appendix B. The trade-offs of low-pass filtering myoelectric control signals

To characterize the performance of amplitude-based myoelectric signals, we investigated the use of alternate low-pass filtering functions of the sEMG data. Three separate low-pass filters were tested: (1) a rectangular window—similar to that used in standard MAV calculations, (2) a Hanning window—to improve the low-pass filtering characteristics, and (3) an asymmetrical window—to test the low-pass filtering characteristics similar to that of a motor unit force twitch. Each window was normalized by its area to achieve DC unity gain and convolved with the rectified sEMG signal. A range of low-pass cutoff frequencies were tested for each filter, corresponding to window lengths ranging from 25 to 500 ms. Examples of the time and frequency domain representations of a 25 ms and 500 ms window for each filter is shown in figure B1 ((A)–(F) and (G)–(L) respectively) and examples of each filtered signals are also shown (figures B1(M)–(R)). Changes in the smoothness and error metrics for different window filter lengths were analyzed as a function of the latency measured by finding the point of maximum cross correlation of each filtered amplitude-based myoelectric signal with respect to the MU Drive signals. (Note that negative latencies indicate the filtered signal leads MU Drive while positive latencies indicate that the filtered signal lags behind MU Drive.) The resulting data was compiled into a single group from all control subjects and all muscles tested.

Results indicated that the rectangular window, similar to that used in standard MAV calculations, achieved a median error of 40.0% (figure B1(S)), a median smoothness of −31.2 (figure B1(V)) and a median latency of 117 ms with respect to MU Drive. When improving the low-pass filtering characteristics using a Hanning window, the median smoothness improved to −2.8 (figure B1(W)) with a similar median latency of 118 ms, but with an increase of the median error to 47.6% (figure B1(T)). By skewing the window asymmetrically to approximate the filtering characteristics of a motor unit force twitch, the median latency with respect to MU Drive was decreased to 0 ms, with a smoothness of −4.3 (figure B1(X)) but with an increased median error of 50.8% (figure B1(U)).

These results demonstrate the inherent trade-off between smoothness, latency and error of sEMG amplitude-based methods of myoelectric control. Specifically, the desired performance of smoothness and error of the filtered sEMG signal is adversely related to the signal latency, with longer duration windows providing improved smoothness and error at the expense of the latency of the response. While changing the window function can improve the smoothness and latency, the resulting filtered signal has increased error with respect to actual kinematics of the intact limb. Because MU Drive is not subjected to the trade-offs inherent to filtered amplitude-based myoelectric signals, it is able to consistently maintain smooth, responsive control signals that better replicate the movement of the intact limb.

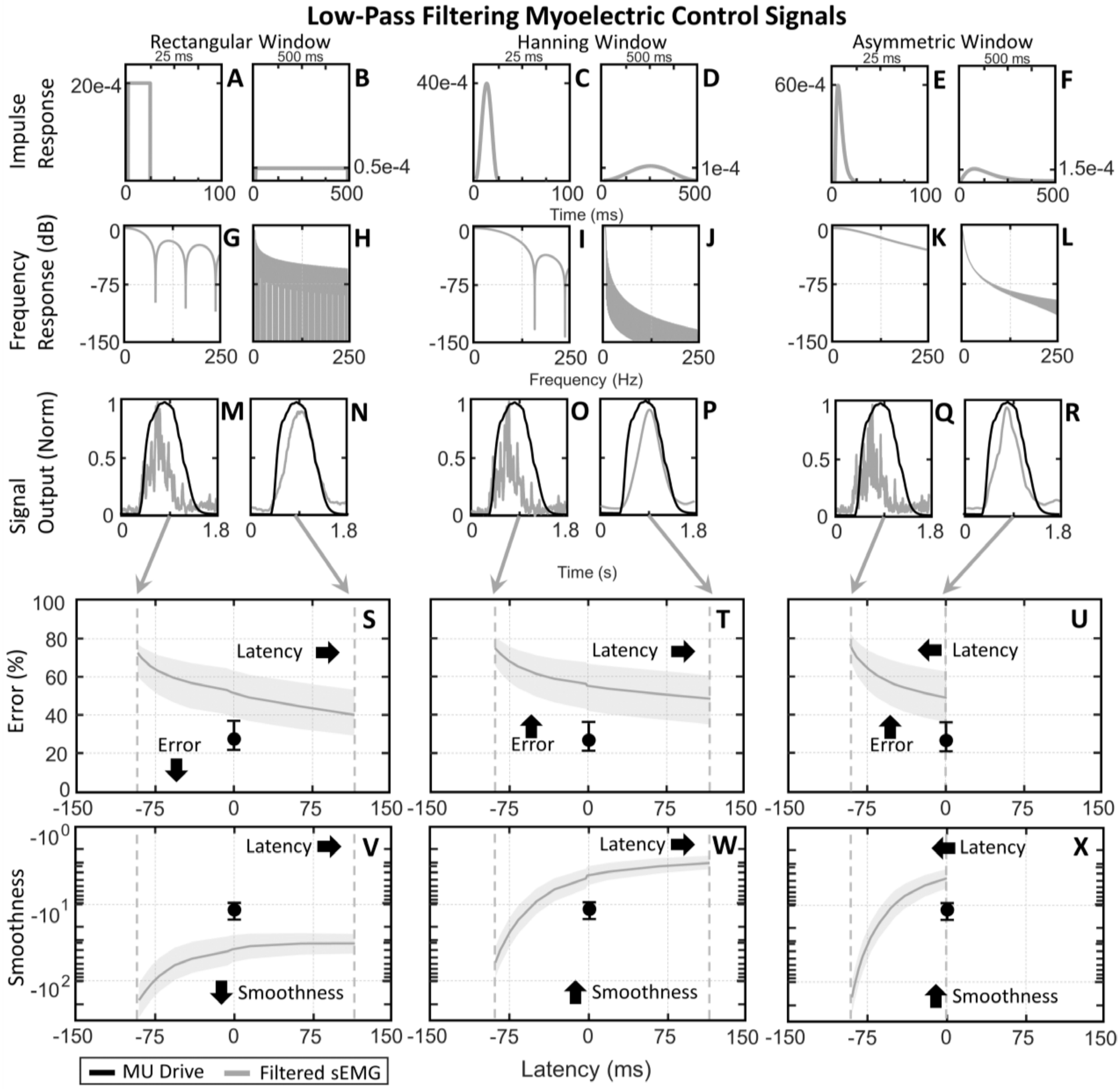

Figure B1. Performance of amplitude-based myoelectric signals low-pass filtered using a rectangular window (S) and (V), a Hanning window (T) and (W), and an asymmetric window (U) and (X) as a function of median latency with respect to MU Drive (black), measured from the finger extensors, the finger flexors, the forearm supinator and the forearm pronator of all control subjects collectively, during finger extension/flexion, forearm supination/pronation. The impulse response of a 25 ms window filter and a 500 ms window filter (A)–(F) is shown, along with their respective frequency responses (G)–(L) and examples of filtered signals (M)–(R). The performance data from MU Drive signals at 25 ms delay are plotted as median values ((S)–(X); black circle) plus and minus the 25th and 75th percentiles ((S)–(X); black error bars). The median error and median smoothness of the amplitude-based signals are represented by the solid traces, while the shaded regions represent the 25th to 75th percentiles. All low-pass filtering techniques demonstrated an inherent trade-off: increasing the duration of the window improves smoothness and error at the expense of latency of the response; whereas changing the window function improves the smoothness and latency, but at the expense of increased error.

ORCID iDs

Michael D Twardowski https://orcid.org/0000-0002-6931-0707
Joshua C Kline https://orcid.org/0000-0002-6523-5527

References

Baker J, Scheme E, Englehart K, Hutchinson D and Greger B 2010 Continuous detection and decoding of dexterous finger flexions with implantable myoelectric sensors *IEEE Trans. Neural Syst. Rehabil. Eng.* **18** 424–32

Balasubramanian S, Melendez-Calderon A, Roby-Brami A and Burdet E 2015 On the analysis of movement smoothness *J. Neuroeng. Rehabil.* **12** 112

Barone U and Merletti R 2013 Design of a portable, intrinsically safe multichannel acquisition system for high-resolution, real-time processing HD-sEMG *IEEE Trans. Biomed. Eng.* **60** 2242–52

Basmajian J and De Luca C 1985 *Muscles Alive: Their Functions Revealed by Electromyography* 5th edn (Baltimore, MD: Williams and Wilkins)

Biddiss E and Chau T 2007 Upper limb prosthesis use and abandonment: a survey of the last 25 years *Prosthet. Orthot. Int.* **31** 236–57

Bowker J and Michael J 1992 *Atlas of Limb Prosthetics* (St. Louis, LA: Mosby)

Clancy E, Bida O and Rancourt D 2006 Influence of advanced electromyogram (EMG) amplitude processors on EMG-to-torque estimation during constant-posture, force-varying contractions *J. Biomech.* **39** 2690–8

Contessa P and De Luca C 2013 Neural control of muscle force: indications from a simulation model *J. Neurophysiol.* **109** 1548–70

Dai C, Bardizbanian B and Clancy E 2017 Comparison of constant-posture force-varying EMG-force dynamic models about the elbow *IEEE Trans. Neural Syst. Rehabil. Eng.* **25** 1529–38

De Luca C 1997 The use of surface electromyography in biomechanics *J. Appl. Biomech.* **13** 135–63

De Luca C and Adam A 1999 Decomposition and analysis of intramuscular electromyographic signals *Modern Techniques in Neuroscience Research* ed U Windhorst and H Johansson (Berlin: Springer) pp 757–76

De Luca C, Adam A, Wotiz R, Gilmore L and Nawab S 2006 Decomposition of surface EMG signals *J. Neurophysiol.* **96** 1646–57

De Luca C, Chang S, Roy S, Kline J and Nawab S 2014 Decomposition of surface EMG signals from cyclic dynamic contractions *J. Neurophysiol.* **113** 1941–51

De Luca C J and Erim Z 1994 Common drive of motor units in regulation of muscle force *Trends Neurosci.* **17** 299–305

Farina D, Vujaklija I, Sartori M, Kapelner T, Negro F, Jiang N, Bergmeister K, Andalib A, Principe J and Aszmann O 2017 Man/machine interface based on the discharge timings of spinal motor neurons after targeted muscle reinnervation *Nat. Biomed. Eng.* **1** 0025

Farrell T and Weir R 2007 The optimal controller delay for myoelectric prostheses *IEEE Trans. Neural Syst. Rehabil. Eng.* **15** 111–8

Fougner A, Stavdahl Ø, Kyberd P, Losier Y and Parker P 2012 Control of upper limb prostheses: terminology and proportional myoelectric control—a review *IEEE Trans. Neural Syst. Rehabil. Eng.* **20** 663–77

Glaser V, Holobar A and Zazula D 2013 Real-time motor unit identification from high-density surface EMG *IEEE Trans. Neural Syst. Rehabil. Eng.* **21** 949–58

Guanglin L, Schultz A and Kuiken T 2010 Quantifying pattern recognition—based myoelectric control of multifunctional transradial prostheses *IEEE Trans. Neural Syst. Rehabil. Eng.* **18** 185–92

Hefferman G, Zhang F, Nunnery M and Huang H 2014 Integration of surface electromyographic sensors with the transfemoral amputee socket: a comparison of four differing configurations *Prosthet. Orthot. Int.* **39** 166–73

Holobar A, Farina D, Gazzoni M, Merletti R and Zazula D 2009 Estimating motor unit discharge patterns from high-density surface electromyogram *Clin. Neurophysiol.* **120** 551–62

Lawrence J and De Luca C 1983 Myoelectric signal versus force relationship in different human muscles *J. Appl. Physiol.* **54** 1653–9

LeFever R and De Luca C 1982 A procedure for decomposing the myoelectric signal into its constituent action potentials—part I: technique, theory, and implementation *IEEE Trans. Biomed. Eng.* **BME-29** 149–57

LeFever R, Xenakis A and De Luca C 1982 A procedure for decomposing the myoelectric signal into its constituent action potentials—part II: execution and test for accuracy *IEEE Trans. Biomed. Eng.* **BME-29** 158–64

Lewis S *et al* 2013 Fully implantable multi-channel measurement system for acquisition of muscle activity *IEEE Trans. Instrum. Meas.* **62** 1972–81

Liu L, Liu P, Clancy E, Scheme E and Englehart K 2013 Electromyogram whitening for improved classification accuracy in upper limb prosthesis control *IEEE Trans. Neural Syst. Rehabil. Eng.* **21** 767–74

Madgwick S, Harrison A and Vaidyanathan R 2011 Estimation of IMU and MARG orientation using a gradient descent algorithm *2011 IEEE Int. Conf. on Rehabilitation Robotics* pp 1–7

Milner-Brown H and Stein R 1975 The relation between the surface electromyogram and muscular force *J. Physiol.* **246** 549–69

Nawab S H, Chang S S and De Luca C J 2010 High-yield decomposition of surface EMG signals *Clin. Neurophysiol.* **121** 1602–15

Pasquina P *et al* 2015 First-in-man demonstration of a fully implanted myoelectric sensors system to control an advanced electromechanical prosthetic hand *J. Neurosci. Methods* **244** 85–93

Phinyomark A, Phukpattaranont P and Limsakul C 2012 Feature reduction and selection for EMG signal classification *Expert Syst. Appl.* **39** 7420–31

Raikova R T and Aladjov H T 2002 Hierarchical genetic algorithm versus static optimization-investigation of elbow flexion and extension movements *J. Biomech.* **35** 1123–35

Reiter R 1948 Eine neue Electrokunsthand *Grenzgebiete Med.* **4** 133–5

Rossini P *et al* 2010 Double nerve intraneural interface implant on a human amputee for robotic hand control *Clin. Neurophysiol.* **121** 777–83

Schorsch J and Weir R 2008 Reliability of implantable myoelectric sensors (IMES) *2008 Virtual Rehabilitation* p 75

Schultz A and Kuiken T 2011 Neural interfaces for control of upper limb prostheses: the state of the art and future possibilities *Phys. Med. Rehabil.* **3** 55–67

Solomonow M, Baratta R and D'Ambrosia R 1991 EMG-force relations of a single skeletal muscle acting across a joint: dependence on joint angle *J. Electromyogr. Kinesiol.* **1** 58–67

Solomonow M, Baratta R, Shoji H and D'Ambrosia R 1990 The EMG-force relationships of skeletal muscle; dependence on contraction rate, and motor units control strategy *Electromyogr. Clin. Neurophysiol.* **30** 141–52